OL Organic Letters

pubs.acs.org/OrgLett Letter

The Challenge of Reproducing with Calculations Raw Experimental Kinetic Data for an Organic Reaction

Raúl Pérez-Soto, Maria Besora,* and Feliu Maseras*

Cite This: https://dx.doi.org/10.1021/acs.orglett.0c00367 Read Online

ACCESS | Metrics & More | Article Recommendations | Supporting Information

ABSTRACT: DFT calculations and microkinetic simulations are applied to the reproduction of previously reported experimental results on the evolution of product concentration versus time in the condensation reaction of *n*-butylamine and benzaldehyde. The mechanism is complicated by the role played by water impurities as proton shuttles. Several functionals and other approaches are tested, yet good agreement is only achieved upon the usage of an adjustment consisting of a directed biasing of the computed DFT free energies.

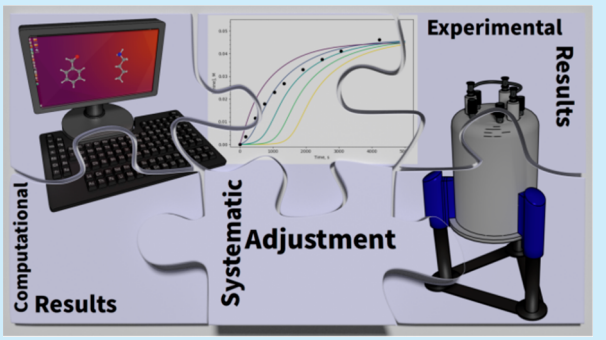

Reproduction, understanding, and prediction of experimental results constitute the main goals of applied computational chemistry. In the early days of computational chemistry, gas phase calculations on molecular models corresponding to minimal representations of the system were performed, and they were able to provide insight about reactions in liquid phase. These early days are long gone, and calculations have now become a widely accepted tool in the determination of mechanisms in organic chemistry.[1−3] In fact, modern computational chemistry, with the available improvements in software and hardware, is now ready to move beyond mechanistic justification and tackle quantitative agreement with many of the experimental measurements.[4] One obvious remaining challenge is the reproduction of raw kinetic data, that is, of the experimentally reported evolution in time of the concentration of the species involved. This is certainly more demanding than reproducing a reaction time or an activation barrier, as has been recently discussed for heterogeneous catalysis,[5] but it can provide a stronger validation for a proposed reaction mechanism.

In this study we set ourselves the goal of reproducing through computational chemistry the kinetic data of a well-known organic reaction, the condensation between an aldehyde and an amine. Specifically, we will try to reproduce the evolution through time of product concentration reported by di Stefano and co-workers for the reaction between benzaldehyde and *n*-butylamine in dichloromethane (Scheme 1).[6]

This condensation reaction has a long history,[7,8] and extensive literature is available on its mechanism, including both experimental[9−11] and computational[12−15] studies. There seems to be a consensus on the mechanism outlined in Scheme 1, with the reaction going through an hemiaminal intermediate. Barriers for the formation of the intermediate are always found to be lower than those for its dehydration. If a direct proton/hydroxyl transfer is considered, prohibitive barriers are found, rendering the inclusion of relay/shuttle molecules mandatory.

Scheme 1. Imine Formation Reaction, Accepted Overall Steps, Intermediate and Experimental Conditions Reproduced in This Work

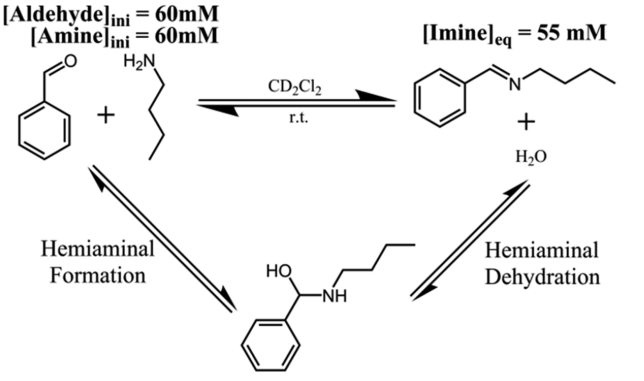

We computed the free energy of all species involved in the mechanism with a rather standard methodology: B3LYP-D3[16−19] with RRHO approximations for free energy corrections, implicit SMD[20] solvation for DCM, and reference

Received: January 28, 2020

https://dx.doi.org/10.1021/acs.orglett.0c00367
Org. Lett. XXXX, XXX, XXX−XXX

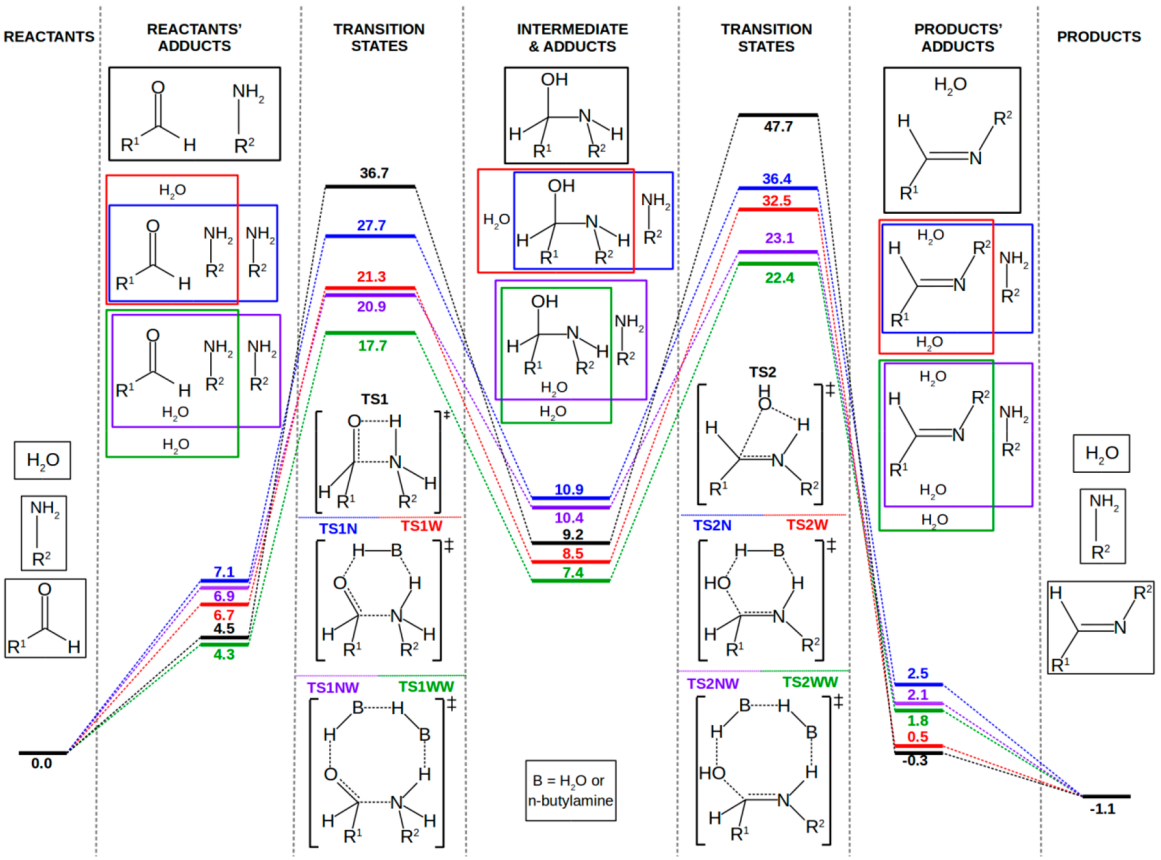

Figure 1. Free energy profiles for the formation of the hemiaminal and the dehydration of the hemiaminal without shuttle (black), a single molecule of water (red), amine (blue), a water dimer (green), or a water-amine adduct (purple). The colored boxes represent the adduct formed by the species enclosed in the box. The colors of these adducts correspond to the step in the free energy profile. Energies are in kcal mol^{-1}.

state corrections[21] for liquid phase at 1 M and 298.15 K. The basis set was cc-pVTZ[22] for all atoms. Unless otherwise stated, all energy calculations were performed using Gaussian09.[23] A data set collection of all computed structures is available in the ioChem-BD repository.[24] Kinetic simulations were carried out using a python script developed in-house. See the Supporting Information (SI) for further details.

The relevant intermediates and transition states computed for the system are included in the free energy profiles in Figure 1. Initially the (formally) simplest mechanism for the noncatalyzed hemiaminal formation and dehydration was calculated (black profile in Figure 1). The obtained barriers (see Figure 1) were clearly too high for a reaction proceeding at room temperature (an overall barrier of 47.7 kcal mol^{-1}). This was to be expected, as the reaction is known to require the presence of catalytic amounts of proton shuttles.

We discarded benzaldehyde and the DCM solvent as potential shuttles because of their low Brønsted acidities. Two other molecules present in the media seem more promising: *n*-butylamine and water, which are generated as side products and are very likely to be present as an impurity from the beginning. We considered them, as well as some possible dimers, as proton shuttles, and this resulted in the other four free energy profiles presented in Figure 1. The results confirm the generally accepted idea on the reaction: the presence of the shuttle can lower the overall barrier to values below 25.0 kcal mol^{-1}, which are far more reasonable. The values of the barriers are indeed comparable to those of previous computational studies and barriers. It is worth mentioning that reactant−shuttle adducts do not correspond to minima in free energy and are thus not isolable. From comparison of the different shuttles, the lowest barrier is achieved with the water dimer (in green), followed by the water−amine adduct (in purple).

The results in Figure 1 and the discussion above follow the general scheme usually applied in computational organic chemistry and provide a qualitatively reasonable picture. The goal of the current work is to go one step further and evaluate the ability of the calculations to reproduce experimentally reported evolution of imine concentration through time. To do so, a microkinetic simulation was carried out using the free energy profiles in Figure 1. We obtained the rate constants from the computed free energy barriers through application of the Eyring equation and used the experimental data as initial concentrations. We considered an initial water impurity of 1 mM which is *ca.* 10 times smaller than the water impurity of Sigma-Aldrich's "100%" deuterated dichloromethane.[25]

The initial results were underwhelming. The evolution of imine concentration according to the direct application of the free energy profiles is included in Figure 2 (purple lines). The product concentration remains negligible (below 10^{-6} M) during the 5000 s of simulated time. The agreement with experiment is poor, as the calculated imine concentration evolution does not resemble the experimental one, represented by the black dots in the figure.

We next considered the adjustment of the DFT results in order to improve agreement with experiment. This technique consists of introducing some small modification in the

https://dx.doi.org/10.1021/acs.orglett.0c00367
Org. Lett. XXXX, XXX, XXX−XXX

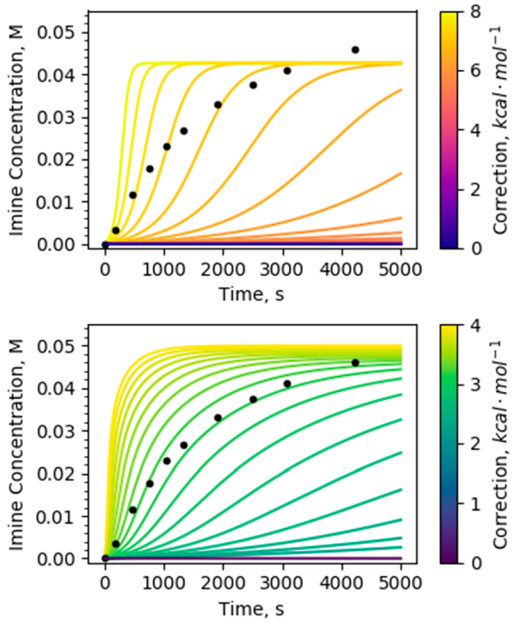

Figure 2. Hypotheses H1 and H2 (above and below respectively) and their effect on the concentration profiles. The plot above corresponds to a systematic and simultaneous reduction of the energies of all transition states in which the C−N and C═N bonds are formed. The plot below corresponds to a systematic and simultaneous increase in the energy of all calculated species.

computed values and has been applied recently with success in computational homogeneous catalysis.[26−28]

We approached the problem by testing two simple hypotheses for adjusting the values in the free energy profiles. The first hypothesis (H1) was "Assume the energies of all TSs are overestimated *X* kcal mol^{-1}", and the second hypothesis (H2) was "Assume that each QM energy has a systematic underestimation of *Y* kcal mol^{-1}". We notice that the change of all QM energies will affect the relative energy of steps involving changes in molecularity. Relative energies remain constant only when the number of molecules remains unchanged. We applied each hypothesis with a wide range of values for the adjustment parameter. The results of their application on the microkinetic simulations are presented in Figure 2. It is clear that hypothesis H1 does not work. On the other hand, the results for hypothesis H2 are very good. We can see that the profile with a "systematic adjustment" of 3.2 kcal mol^{-1} provides a good fit to the experimental values.

After the adjustment, our results are consistent with the observed kinetics of product formation. Moreover, the simulation also gives information on the evolution of the concentrations of all species involved in the reaction. The qualitative picture is that the steps through transition states TS2NW and TS2WW control the overall kinetics (purple and green path respectively in Figure 1). In a first stage the reaction is controlled by TS2NW, and as time passes and water concentration increases TS2WW starts to gain control. This shift is due to the concentration effects, which is a major result of the microkinetic simulations not achievable by the traditional free energy profiles. A more detailed discussion is provided in the SI.

The main result of this work is the validation of the concept that raw kinetic data can be reproduced from computational data by using an adjustment of the computed free energy profiles. We cannot answer at this point why this specific adjustment and why this particular value. This may be related to the controversial issue of entropy corrections in solution, which we have recently discussed elsewhere.[29] In this sense, we can also add that a 3.2 kcal mol^{-1} correction is quite smaller than those proposed by most commonly used treatments.

For the sake of completeness, we examined the possibility of "improving" the kinetic model or the free energy profile without using the adjustment reported above. We computed free energy profiles with BP86-D3, PBEPBE-D3 (generally known as PBE0-D3), PBE1PBE-D3, M06-D3, M06-2X-D3, and ωB97X-D. From those, PBEPBE-D3 and M06-2X-D3 were chosen to run microkinetic simulations, yet B3LYP-D3 stood as the best fit (see SI).

We carried out a final attempt to obtain better energies by using the DLPNO-CCSD(T)[30] method, with corresponding matching auxiliary basis functions, Tight SCF cutoff, and Normal PNO defaults, as implemented in the ORCA4.0 package.[31] To our surprise, the agreement with experiment was substantially worse than with B3LYP-D3. Table 1 collects

Table 1. Effect of Solvation in the Potential Energy[a]

	B3LYP-D3/cc-pVTZ		DLPNO/cc-pVTZ	
species	ΔE_{vac}	$\Delta E_{smd} - \Delta E_{vac}$	ΔE_{vac}	$\Delta E_{smd} - \Delta E_{vac}$
TS2	43.0	−5.5	52.2	−7.1
TS2W	20.8	−6.0	29.7	−6.4
TS2N	16.2	0.5	20.2	1.3
TS2WW	−10.5	4.6	0.3	4.7
TS2NW	−5.2	3.1	5.2	3.7
Hemiaminal	−5.7	1.8	−8.9	2.1
Imine + Water	0.2	−1.2	−2.7	−0.5

[a]Energies in kcal mol^{-1}. Single-point calculations on B3LYP-D3/cc-pVTZ geometries optimized in solvent.

some potential (referred by some as electronic) energy values for selected points in the potential energy surface. The DLPNO-CCSD(T) values for potential energy barriers in vacuum are *ca.* 10 kcal mol^{-1} higher than the B3LYP-D3 values. This result was not modified by extensions of the basis set to cc-pVQZ or cc-pV5Z (see SI). Solvation effects are significant, as expected for these systems containing electrostatic interactions, but the relative effect of the solvation $\Delta E_{smd} - \Delta E_{vac}$ is similar for both methods and cannot compensate the change in potential energy. Therefore, DLPNO-CCSD(T) barrier heights taken at face value render the calculated mechanism much slower, which is not compatible with experiment.

We definitely trust DLPNO-CCSD(T) gas phase potential energies more than the B3LYP-D3 ones. Thus, we are skeptical of the effect of solvation on the relative energies, which is also reported in Table 1. It might be argued that due to experimental information contained in the fitting of DFT functionals, SMD might be better at reproducing the solvent-phase potential energy surface with B3LYP-D3. We are not sure how to interpret this DLPNO-CCSD(T) result, but we think it is important to put forward a word of caution for cases where high accuracy in solution is required.

In summary, we have shown that modern computational chemistry is able to reproduce raw kinetic data for an organic process using pure theoretical values, but that the treatment remains far from trivial even for a relatively simple process such as the condensation of an aldehyde and an amine to form an

https://dx.doi.org/10.1021/acs.orglett.0c00367
Org. Lett. XXXX, XXX, XXX−XXX

imine. The usage of a kinetic model is nicely complemented by the use of a relatively minor *a posteriori* adjustment of the computed free energy values. This energy adjustment coupled with simulations is a possible solution to fill the gap between computational end experimental results. Further work will be necessary to confirm the general validity of these results, but the results look promising for a further expansion of the application of computational chemistry.

■ ASSOCIATED CONTENT

Supporting Information

The Supporting Information is available free of charge at https://pubs.acs.org/doi/10.1021/acs.orglett.0c00367.

Computational details, free energies from the DFT and DLPNO-CCSD(T) benchmarks, the microkinetic model simulation details as well as the potential energy, Cartesian coordinates, and number of imaginary frequencies for all reported stationary points (PDF)

■ AUTHOR INFORMATION

Corresponding Authors

Maria Besora − *Departament de Química Física i Inorgànica, Universitat Rovira i Virgili, 43007 Tarragona, Catalonia, Spain;* orcid.org/0000-0002-6656-5827; Email: maria.besora@urv.cat

Feliu Maseras − *Institute of Chemical Research of Catalonia (ICIQ), The Barcelona Institute of Science and Technology, 43007 Tarragona, Catalonia, Spain;* orcid.org/0000-0001-8806-2019; Email: fmaseras@iciq.es

Author

Raúl Pérez-Soto − *Institute of Chemical Research of Catalonia (ICIQ), The Barcelona Institute of Science and Technology, 43007 Tarragona, Catalonia, Spain;* orcid.org/0000-0002-6237-2155

Complete contact information is available at: https://pubs.acs.org/10.1021/acs.orglett.0c00367

Notes

The authors declare no competing financial interest.

■ ACKNOWLEDGMENTS

This work was supported by the Spanish MINECO, Ministerio de Economía, Industria y Competitividad, (CTQ2017-87792-R) and the CERCA Programme of the Generalitat de Catalunya. R.P.-S. holds an FPU grant (Formacion de Profesorado Universitario) from the MCIU, Ministerio de Ciencia y Innovacion y Universidades (FPU18/01138).

■ REFERENCES

(1) Shu, C.; Wang, Y.-H.; Shen, C.-H.; Ruan, P.-P.; Lu, X.; Ye, L.-W. Gold-Catalyzed Intermolecular Ynamide Amination-Initiated Aza-Nazarov Cylization: Access to Functionalized 2-Aminopyrroles. *Org. Lett.* **2016**, *18*, 3254−3257.

(2) Genovino, J.; Lian, Y.; Zhang, Y.; Hope, T. O.; Juneau, A.; Gagné, Y.; Ingle, G.; Frenette, M. Metal-Free-Visible Light C-H Alkylation of Heteroaromatics via Hypervalent Iodine-Promoted Decarboxylation. *Org. Lett.* **2018**, *20*, 3229−3232.

(3) Wang, S.; Rodríguez-Escrich, C.; Fianchini, M.; Maseras, F.; Pericàs, M. A. Diasterodivergent Enantioselective [8 + 2] Annulation of Tropones and Enals Catalyzed by N-Heterocylic Carbenes. *Org. Lett.* **2019**, *21*, 3187−3192.

(4) Harvey, J. N.; Himo, F.; Maseras, F.; Perrin, L. Scope and Challenge of Computational Methods for Studying Mechanism and Reactivity in Homogeneous Catalysis. *ACS Catal.* **2019**, *9*, 6803−6813.

(5) Matera, S.; Schneider, W. F.; Heyden, A.; Savara, A. Progress in Accurate Chemical Kinetic Modeling, Simulations, and Parameter Estimation for Heterogeneous Catalysis. *ACS Catal.* **2019**, *9*, 6624−6647.

(6) Ciaccia, M.; Cacciapaglia, R.; Mencarelli, P.; Mandolini, L.; di Stefano, S. Fast transimination in organic solvents in the absence of proton and metal catalysts. A key to imine metathesis catalyzed by primary amines under mild conditions. *Chem. Sci.* **2013**, *4*, 2253−2261.

(7) Schiff, H. Mittheilungen aus dem Universitätslaboratorium in Pisa: Eine neue Reihe organischer Basen. *Justus Liebigs Ann. Chem.* **1864**, *131*, 118−119.

(8) Sprung, M. A. A Summary of the Reactions of Aldehydes with Amines. *Chem. Rev.* **1940**, *26*, 297−338.

(9) Sayer, J. M.; Jencks, W. P. Imine-Forming Elimination Reactions. 2. Imbalance of Charge Distribution in the Transition State for Carbinolamine Dehydration. *J. Am. Chem. Soc.* **1977**, *99*, 464−474.

(10) Qin, W.; Long, S.; Panunzio, M.; Biondi, S. Schiff Bases: A Short Survey on an Evergreen Chemistry Tool. *Molecules* **2013**, *18*, 12264−12289.

(11) Ciaccia, M.; di Stefano, S. Mechanisms of imine exchange reactions in organic solvents. *Org. Biomol. Chem.* **2015**, *13*, 646−654.

(12) Casasnovas, R.; Adrover, M.; Ortega-Castro, J.; Frau, J.; Donoso, J.; Muñoz, F. C-H. Activation in Pyridoxal-5′-phosphate Schiff Bases: The Role of the Imine Nitrogen. A Combined Experimental and Computational Study. *J. Phys. Chem. B* **2012**, *116*, 10665−10675.

(13) Calow, A. D. J.; Carbó, J. J.; Cid, J.; Fernandez, E.; Whiting, A. Understanding α,β-Unsaturated Imine Formation from Amine Additions to α,β-Unsaturated Aldehydes and Ketones: An Analytical and Theoretical Investigation. *J. Org. Chem.* **2014**, *79*, 5163−5172.

(14) Boz, E.; Tüzün, N. Ş.; Stein, M. Computational investigation of the control of the thermodynamics and microkinetics of the reductive amination reaction by solvent coordination and co-catalyst. *RSC Adv.* **2018**, *8*, 36662.

(15) Sheng, X.; Himo, F. Enzymatic Pictet-Spengler Reaction: Computational Study of the Mechanism and Enantioselectivity of Norcoclaurine Synthase. *J. Am. Chem. Soc.* **2019**, *141*, 11230−11238.

(16) Stephens, P. J.; Devlin, F. J.; Chabalowski, C. F.; Frisch, M. J. Ab Initio Calculation of Vibrational Absorption and Circular Dichroism Spectra Using Density Functional Force Fields. *J. Phys. Chem.* **1994**, *98*, 11623−11627.

(17) Lee, C.; Yang, W.; Parr, R. G. Development of the Colle-Salvetti correlation-energy formula into a functional of the electron density. *Phys. Rev. B: Condens. Matter Mater. Phys.* **1988**, *37*, 785−789.

(18) Becke, A. D. Density-functional thermochemistry. III. The role of exact exchange. *J. Chem. Phys.* **1993**, *98*, 5648−5652.

(19) Grimme, S. Semiempirical GGA-type density functional constructed with a long-range dispersion correction. *J. Comput. Chem.* **2006**, *27*, 1787−1799.

(20) Marenich, A. V.; Cramer, C. J.; Truhlar, D. G. Universal Solvation Model Based on Solute Electron Density and on a Continuum Model of the Solvent Defined by the Bulk Dielectric Constant and Atomic Surface Tensions. *J. Phys. Chem. B* **2009**, *113*, 6378−6396.

(21) Ribeiro, R. F.; Marenich, A. V.; Cramer, C. J.; Truhlar, D. G. Use of Solution-Phase Vibrational Frequencies in Continuum Models for the Free Energy of Solvation. *J. Phys. Chem. B* **2011**, *115*, 14556−14562.

(22) Dunning, T. H., Jr. Gaussian basis sets for use in correlated molecular calculations. I. The atoms boron through neon and hydrogen. *J. Chem. Phys.* **1989**, *90*, 1007.

(23) Frisch, M. J.; Trucks, G. W.; Schlegel, H. B.; Scuseria, G. E.; Robb, M. A.; Cheeseman, J. R.; Scalmani, G.; Barone, V.; Mennucci, B.; Petersson, G. A.; Nakatsuji, H.; Caricato, M.; Li, X.; Hratchian, H.

P.; Izmaylov, A. F.; Bloino, J.; Zheng, G.; Sonnenberg, J. L.; Hada, M.; Ehara, M.; Toyota, K.; Fukuda, R.; Hasegawa, J.; Ishida, M.; Nakajima, T.; Honda, Y.; Kitao, O.; Nakai, H.; Vreven, T.; Montgomery, J. A., Jr.; Peralta, J. E.; Ogliaro, F.; Bearpark, M.; Heyd, J. J.; Brothers, E.; Kudin, K. N.; Staroverov, V. N.; Keith, T.; Kobayashi, R.; Normand, J.; Raghavachari, K.; Rendell, A.; Burant, J. C.; Iyengar, S. S.; Tomasi, J.; Cossi, M.; Rega, N.; Millam, J. M.; Klene, M.; Knox, J. E.; Cross, J. B.; Bakken, V.; Adamo, C.; Jaramillo, J.; Gomperts, R.; Stratmann, R. E.; Yazyev, O.; Austin, A. J.; Cammi, R.; Pomelli, C.; Ochterski, J. W.; Martin, R. L.; Morokuma, K.; Zakrzewski, V. G.; Voth, G. A.; Salvador, P.; Dannenberg, J. J.; Dapprich, S.; Daniels, A. D.; Farkas, O.; Foresman, J. B.; Ortiz, J. V.; Cioslowski, J.; Fox, D. J. *Gaussian 09*, revision D.01; Gaussian, Inc.: Wallingford, CT, 2013.

(24) Álvarez-Moreno, M.; de Graaf, C.; López, N.; Maseras, F.; Poblet, J. M.; Bo, C. Managing the Computational Chemistry Big Data Problem: The ioChem-BD Platform. *J. Chem. Inf. Model.* **2015**, *55*, 95−103.

(25) *Sigma Aldrich webpage. Specification sheet, product 237027*. https://www.sigmaaldrich.com/catalog/product/aldrich/237027 (accessed Dec 20, 2019).

(26) Artús Suàrez, L.; Culakova, Z.; Balcells, D.; Bernskoetter, W. H.; Eisenstein, O.; Goldberg, K. I.; Hazari, N.; Tilset, M.; Nova, A. The Key Role of the Hemiaminal Intermediate in the Iron-Catalyzed Deaminative Hydrogenation of Amides. *ACS Catal.* **2018**, *8*, 8751−8762.

(27) Yu, Y.; Zhu, Y.; Bhagat, M. N.; Raghuraman, A.; Hirsekorn, K. F.; Notestein, J. M.; Nguyen, S. T.; Broadbelt, L. J. Mechanism of Regioselective Ring-Opening Reactions of 1,2-Epoxyoctane Catalyzed by Tris(pentafluorphenyl)borane): A Combined Experimental, Density Functional Theory and Microkinetic Study. *ACS Catal.* **2018**, *8*, 11119−11133.

(28) Jaraíz, M.; Rubio, J. E.; Enríquez, L.; Pinacho, R.; López-Pérez, J. L.; Lesarri, A. An Efficient Microkinetic Modeling Protocol: Start with Only the Dominant Mechanisms, Adjust All Parameters, and Build the Complete Model Incrementally. *ACS Catal.* **2019**, *9*, 4804−4809.

(29) Besora, M.; Vidossich, P.; Lledós, A.; Ujaque, G.; Maseras, F. Calculation of Free Energies in Solution: A Comparison of Current Approaches. *J. Phys. Chem. A* **2018**, *122*, 1392−1399.

(30) Riplinger, C.; Neese, F. An Efficient and near linear scaling pair natural orbital based local coupled cluster method. *J. Chem. Phys.* **2013**, *138*, 034106.

(31) Neese, F. Software update: the ORCA program system, version 4.0. *Wiley Interdiscip. Rev.: Comput. Mol. Sci.* **2018**, *8*, No. e1327.

https://dx.doi.org/10.1021/acs.orglett.0c00367
Org. Lett. XXXX, XXX, XXX−XXX